

Nonlocality effect in the tunneling of one-proton radioactivity

N. Teruya

Departamento de Física, Universidade Federal da Paraíba - UFPB Campus de João Pessoa, 58051-970, João Pessoa - PB, Brazil

S. B. Duarte and M. M. N. Rodrigues

Centro Brasileiro de Pesquisas Físicas-CBPF/MCTI Rua Dr. Xavier Sigaud, 150, 22290-180, Rio de Janeiro-RJ, Brazil

(Received 15 September 2015; published 3 February 2016)

A coordinate-dependent effective mass for the proton is considered to calculate half-lives of spontaneous one-proton emission from exotic nuclei. This dynamical change to treat proton-nucleus interaction using this type of effective mass was recently employed successfully for description of proton-nucleus quantum scattering, by Jaghoub *et al.* [*Phys. Rev. C* **84**, 034618 (2011)] and Zureikat and Jaghoub [*Nucl. Phys. A* **916**, 183 (2013)]. The introduced coordinate dependency of the effective mass incorporates nonlocality features of the proton-nucleus interaction for the scattering problem. In the present work the treatment is extended to the proton emission of neutron deficient nuclei. The WKB barrier penetrability factor is determined for proton decay and the half-life is calculated. It is also shown that the tunneling approach is still applicable when a coordinate-dependent effective mass is considered. The real part of the Becchetti and Greenlees [*Phys. Rev.* **182**, 1190 (1969)] nuclear shell model parametrization is taken to generate the barrier tunneled by the proton. This procedure leads practically to only one free parameter in the effective mass for the entire calculation of the half-lives of the whole set of existing almost spherical proton emitters. In the universe of 32 proton emitters studied we have obtained an excellent agreement for 25 of them, while for the remaining seven emitters it was necessary to add an additional fine tuning, realized by a small change in the nuclear radius parameter definition.

DOI: [10.1103/PhysRevC.93.024606](https://doi.org/10.1103/PhysRevC.93.024606)

I. INTRODUCTION

The proton radioactivity phenomenon has attracted attention as an important tool for the understanding of the nuclear structure of nuclides far from the stability line. Different theoretical approaches have been proposed to elucidate the proton decay mechanism of neutron deficient nuclear systems [1,2]. However, no conclusive decision on the appropriate nuclear model to describe the decay process has been reached yet. Phenomenological treatments in conjunction with the experimental effort [2–4] (and references therein) have been used to enlighten the theoretical treatment of proton emission from exotic nuclei. In addition, systematic studies have been accompanied by these studies which aim at predicting new possibilities of emitters, in order to clarify the phenomenon [5]. The currently proposed models treat the parent nucleus as a single proton orbiting an inert core, and the decay half-life is evaluated by considering it as a quasistationary state.

Besides the difficulties inherent to the determination of the complete microscopic structure of these highly unstable nuclei [6–9], on the theoretical side some essential aspects of the decay process are still unexplored. Examples of this are the role of Pauli blocking in the proton-nucleus interaction, as well as the nonlocality feature of proton-nucleus interaction. There is some room to include these aspects in a model for half-lives calculation which is pointed out in the present work.

The discussion concerning the nonlocality of particle interaction with nuclei has been pursued since the pioneering work by Feshbach [10] and by Frahn and Lemmer [11] in the context of nucleon-nucleus scattering studies. This problem requires a careful analysis both in relativistic [12] and nonrelativistic contexts [10,11,13–15]. With the coordinate dependency of the particle mass a new form of the kinetic energy operator

should be constructed in order to preserve the Hermitian character of the operator. At first glance the uniqueness of the operator is not guaranteed (see detailed discussion in Refs. [14,16]). However, one must consider that the continuity of the derivative of the proton wave function at boundaries with abrupt interfaces enables a restricted choice for the kinetic Hamiltonian form of the Schrödinger treatment [17]. Thus, these works show that a coordinate dependence of the proton effective mass consistently incorporates a non-locality effect in the quantum description for the proton interaction with the nucleus. This aspect was not taken into account in previous determinations of half-lives of observed proton emitters. More recently, a nonlocality effect was successfully used to solve problems arising in the adjustment of proton-nucleus scattering differential cross section by Zureikat and Jaghoub [14]. At this point it is important to clarify that concurrently nonlocality effect is characterized by the introduction of an energy or velocity dependence in potential when dealing with the proton-nucleus scattering problem [18–22]. As we will see later, this velocity or energy dependence also arises when consistently considering the coordinate dependence of the effective mass.

In the present work we report on results obtained from a half-lives calculation of proton emitters, using the coordinate-dependent effective mass in a typical nuclear shell model potential barrier, tunneled by the proton. The next section details the used potential barrier construction. Section III details the effective mass expression and the extension of the WKB method to calculate barrier penetrability for the case of coordinate-dependent effective mass. Our results and discussions are presented in Sec. IV. Conclusions and final remarks are in the last section.

II. THE HALF-LIFE DETERMINATION AND POTENTIAL BARRIER CONSTRUCTION

Half-lives of one proton emission from the ground state and metastable isomeric nuclear state of neutron deficient nuclei with $A \geq 144$ are determined by using the WKB approximation to calculate the barrier penetrability factor. Within this approximation we have for the half-life T and the decay constant λ ,

$$T = \frac{\ln(2)}{\lambda}; \quad \lambda = \lambda_0 e^{-G}, \quad (1)$$

where G is the Gamow's factor through the barrier and λ_0 is the ratio for proton assault to the potential barrier. For a proton decay with angular momentum ℓ we have [23]

$$\lambda_0 = \sqrt{\frac{(Q_p - V_{\min})(1 + \delta_{l0})}{4\mu(R_2 - R_1)^2}}, \quad (2)$$

where the symbol δ_{l0} is the Kronecker's delta and V_{\min} corresponds to the minimum value of the potential well in Fig. 1(b). The distances R_1 and R_2 locate the classical turning points adjacent to the potential well, and R_3 is the external one in the descendent region of the barrier. The reduced mass of the system $p + \text{core}$ is μ and the Q_p value is the decay energy. The Gamow's factor of the penetrability in Eq. (1) is calculated as

$$G = \frac{2}{\hbar} \int_{R_2}^{R_3} \sqrt{2\mu [V(r) - Q_p]} dr, \quad (3)$$

where $V(r)$ is the total shell model potential, accounting for the sum of the nuclear Woods-Saxon potential V_{WS} with the spin-orbit V_{LS} , Coulomb V_C , and the centrifugal potential energies V_L ,

$$V(r) = V_{WS}(r) + V_{LS}(r) + V_C(r) + V_L(r), \quad (4)$$

with

$$V_{WS}(r) = -\frac{V_0}{1 + \exp[(r - R)/a]}, \quad (5)$$

in which V_0 is the nuclear potential depth, R is the nuclear radius calculated as $R = r_0 A^{1/3}$ and a is the potential diffusivity parameter.

The spin-orbit potential is taken as

$$V_{LS}(r) = V_{so} \lambda_\pi^2 (\vec{l} \cdot \vec{\sigma}) \frac{1}{r} \frac{d}{dr} [f(r, R_{so}, a_{so})], \quad (6)$$

where $f(r, R_{so}, a_{so}) = \{1 + \exp[(r - R_{so})/a_{so}]\}^{-1}$. The scalar product of the intrinsic and orbital angular momentum operator, $\vec{l} \cdot \vec{\sigma}$, is calculated as

$$\vec{l} \cdot \vec{\sigma} = \begin{cases} -(\ell + 1); & \text{for } j = \ell - 1/2 > 0 \\ \ell; & \text{for } j = \ell + 1/2 \end{cases}, \quad (7)$$

where j and ℓ are the total and orbital angular momentum quantum numbers for the emitted proton. The depth of spin-orbit potential is fixed at $V_{so} = 6.2$ MeV; the value for the diffusivity parameters a_{ls} is set equal to 0.75 fm. The pion Compton wavelength squared which appears in the spin-orbit

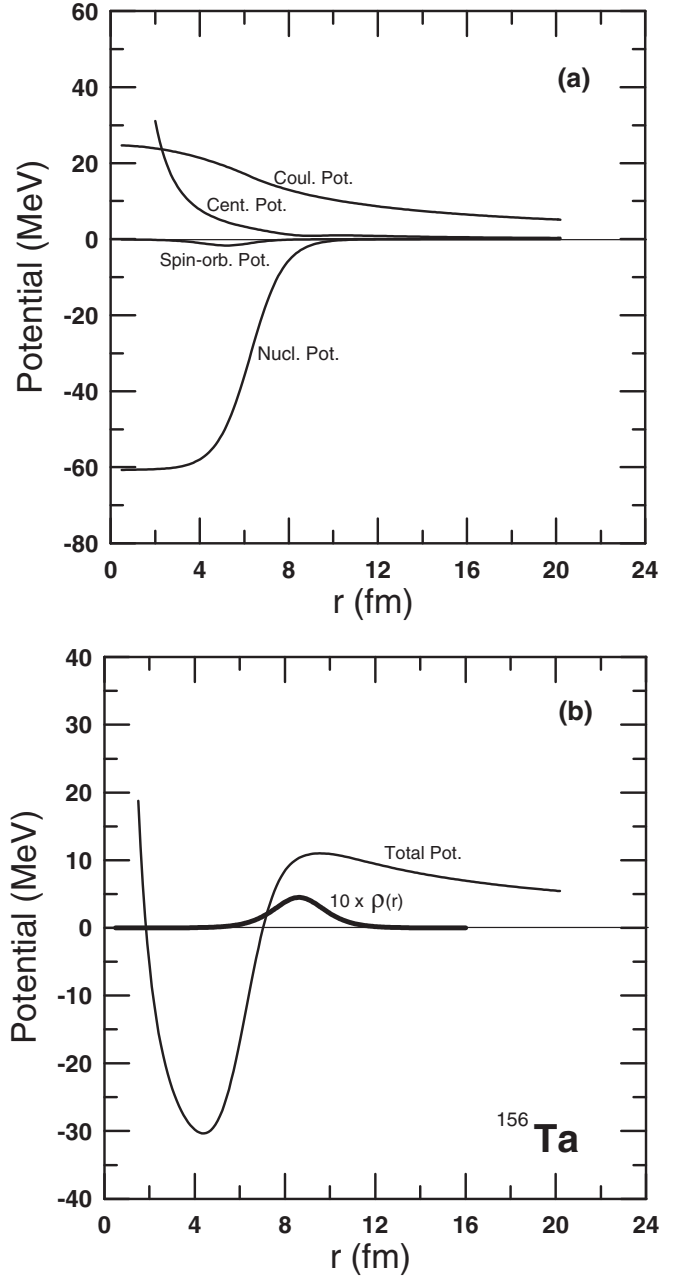


FIG. 1. Illustrated in (a) is the different terms of the nuclear potential for the case of ^{156}Ta proton emitter. (b) displays the total potential and illustrates the behavior of the dimensionless function $\rho(r)$ of Eq. (11). This latter is multiplied by a factor ten to display both plots in the same graphic scale.

term was taken as $\lambda_\pi^2 = 2.14 \text{ fm}^2$ and R_{so} is calculated as $R_{so} = r_{0,so} A^{1/3}$ with $r_{0,so} = 1.01 \text{ fm}$.

The Coulomb potential is calculated as

$$V_C(r) = \begin{cases} Z_d e^2 / r; & r > R \\ Z_d e^2 [3 - (r/R)^2] / 2R; & r \leq R \end{cases}, \quad (8)$$

where Z_d is the atomic number of the daughter nucleus and e^2 is the electron charge squared.

For the centrifugal term we have

$$V_L(r) = \frac{\ell(\ell+1)\hbar^2}{2\mu r^2} \quad (9)$$

The parameters of the potential $V(r)$ have standard values taken from Becchetti's parametrization in Ref. [24]. The nuclear radius in the calculation is given by $R = r_0 A^{1/3}$, with μ being the reduced mass of the decaying system, which is calculated using the coordinate-dependent effective mass $m(r)$ for the proton mass as described in next section.

III. THE COORDINATE-DEPENDENT EFFECTIVE MASS AND TUNNELING CALCULATION

The coordinate-dependent proton effective mass was recently employed to solve problems in the study of elastic nucleon-nucleus scattering process in Refs. [13,14]. For a spherically symmetric proton-nucleus interaction the effective mass is properly described by

$$m = \frac{m_0}{1 - \rho(r)}, \quad (10)$$

with

$$\rho(r) = \rho_s a_s \frac{d}{dr} \left[1 + \exp\left(\frac{r - R_s}{a_s}\right) \right]^{-1}, \quad (11)$$

where R_s and a_s are parameters associated to the centroid location and width of effective mass function, respectively, illustrated in Fig. 1(b). In our calculation we take $R_s = R + 2$ fm and $a_s = a$; these values are in accordance with those in Refs. [13,14].

Our purpose here is to apply the WKB approximation to determine the proton emission half-lives. At this point, since the proton effective mass is now a function of the distance r it is necessary to show that the expression of the Gamow's factor in Eq. (3) can be maintained. For this the above effective mass expression can be substituted in the Schrödinger equation for the proton emission problem,

$$\begin{aligned} & -\frac{\hbar^2}{2m} \left\{ \frac{d^2}{dr^2} - \frac{1}{m} \frac{dm}{dr} \left[\frac{d}{dr} - \frac{1}{r} \right] - \frac{\ell(\ell+1)}{r^2} \right\} \Psi \\ & = (E - V_{\text{int}}) \Psi, \end{aligned} \quad (12)$$

where V_{int} is the central potential of the interaction.

We put the centrifugal term in the other side of equality, defining the new potential term, \tilde{V} , given by

$$\tilde{V} = V_{\text{int}} + \frac{\ell(\ell+1)\hbar^2}{2m r^2}. \quad (13)$$

Also we replace Eqs. (13) and (10) in Eq. (12),

$$-\frac{\hbar^2}{2m_0} (1 - \rho) \left\{ \frac{d^2 \Psi}{dr^2} - \frac{1}{1 - \rho} \frac{d\rho}{dr} \left[\frac{d\Psi}{dr} - \frac{\Psi}{r} \right] \right\} = (E - \tilde{V}) \Psi. \quad (14)$$

Now by taking the standard semiclassical solution of stationary phase as the usual WKB approximation,

$$\Psi = N e^{i\phi(r)/\hbar}. \quad (15)$$

After some algebra Eq. (12) becomes

$$\begin{aligned} & -\frac{1}{2m_0} \left\{ (1 - \rho) i \hbar \frac{d^2 \phi}{dr^2} - (1 - \rho) \left(\frac{d\phi}{dr} \right)^2 \right\} \\ & + \frac{1}{2m_0} \left\{ \frac{d\rho}{dr} \left(i \hbar \frac{d\phi}{dr} + \frac{\hbar^2}{r} \right) \right\} = (E - \tilde{V}). \end{aligned} \quad (16)$$

Considering the terms that have first power of \hbar we obtain

$$\frac{1 - \rho}{2m_0} \left(\frac{d\phi}{dr} \right)^2 = (E - \tilde{V}). \quad (17)$$

Finally, we get

$$\frac{d\phi}{dr} = \sqrt{2m(r)(E - \tilde{V})} \quad (18)$$

and

$$\phi(r) = \int \sqrt{2m(r)(E - \tilde{V})} dr. \quad (19)$$

This is the same form of the Gamow penetrability factor for the constant mass problem, only changing $m \rightarrow m(r)$. We call attention to the fact that in Eq. (12) the term with the first-order derivative can be viewed as a velocity-dependent potential term in the Schrödinger equation of the decay process. This term comes from the procedure to redefine the proton kinetic energy as a Hermitian operator when the effective mass is dependent on the proton position [13,14].

IV. RESULTS AND CONCLUDING REMARKS

To illustrate the contribution of the potential terms to the barrier formation see part (a) of Fig. 1 which displays a plot of these terms to the case of ^{156}Ta proton emitter. The behavior of the barrier and of the function $\rho(r)$ in Eq. (11) are shown in part (b). Note that variations in the function $\rho(r)$ are relevant only at the nuclear surface region.

By using Eqs. (1)–(9) we have calculated half-lives of 32 proton emitters with $A \geq 144$. Firstly, we did the calculation without the use of the nonlocality effect, taking the proton free mass value, as it is currently done in the literature. The purpose of this is to verify if the chosen potential barrier model is able to offer reasonable half-life values for the set of almost spherical emitters ($|\beta_2| \leq 0.258$, where β_2 is the deformation parameter used in Ref. [1]). The results are shown as $T_{\text{FM}}^{\text{cal}}$ values in Tables I and II. To verify if these results are reasonable enough the standard deviation in respect to data was calculated by

$$\sigma_s = \sqrt{\frac{1}{n-2} \sum_{i=1}^n \left[\log \left(\frac{T_{\text{FM}}^{\text{cal}}(i)}{T^{\text{exp}}(i)} \right) \right]^2} \quad (20)$$

with $T_{\text{FM}}^{\text{cal}}(i)$ and $T^{\text{exp}}(i)$ being the calculated and experimental half-lives of i th emitter, respectively. This standard deviation of half-lives calculated for the 32 emitters is $\sigma_s \cong 0.66$ with values in Tables I and II. The same calculation restricted to the set of 25 emitters in Table I is reduced to $\sigma_s \cong 0.48$. The reached degree of data accordance is comparable with the best results of calculations in the literature.

The significant disagreement between the model prediction and data occurs for the seven emitters separated in Table II. In

TABLE I. This table shows the proton emitters nuclei (first column), the nuclear potential depth [in Eq. (5)] using Becchetti's parametrization for the proton-nucleus interaction [24] is shown in the second column. In the third column are the calculated half-lives without effective correction, that means by using free mass (FM). The fourth column is for the half-lives with the proton effective mass (EM) correction. In the last column is shown the best values of the effective mass parameter in Eq. (11). The value of $r_0 = 1.17$ fm was maintained for the half-life calculation of all emitters in this table. The values of experimental half-lives and other data inputs for the calculation, such as angular moment, total angular moment, and decay energy Q , were taken from the compilation in Ref. [1].

Nucleus	V_0^{Bech} (MeV)	$T_{\text{FM}}^{\text{calc}}$ (s)	$T_{\text{EM}}^{\text{calc}}$ (s)	ρ_s
$^{144}_{69}\text{Tm}$	59.824	2.463×10^{-6}	2.724×10^{-6}	-0.52
$^{145}_{69}\text{Tm}$	59.961	1.546×10^{-6}	3.486×10^{-6}	-2.42
$^{146}_{69}\text{Tm}$	60.280	5.490×10^{-2}	1.186×10^{-1}	-2.26
$^{147}_{69}\text{Tm}$	60.466	2.425×10^0	3.796×10^0	-1.60
$^{147m}_{69}\text{Tm}$	60.447	1.806×10^{-4}	3.596×10^{-4}	-1.59
$^{150}_{71}\text{Lu}$	60.321	3.068×10^{-2}	6.431×10^{-2}	-2.17
$^{150m}_{71}\text{Lu}$	60.313	9.155×10^{-6}	4.301×10^{-5}	-2.64
$^{151}_{71}\text{Lu}$	60.469	6.131×10^{-2}	1.272×10^{-1}	-2.15
$^{151m}_{71}\text{Lu}$	60.444	4.916×10^{-6}	1.609×10^{-5}	-2.28
$^{155}_{73}\text{Ta}$	60.462	1.562×10^{-3}	2.912×10^{-3}	-1.94
$^{156}_{73}\text{Ta}$	60.734	6.410×10^{-2}	1.494×10^{-1}	-1.80
$^{156m}_{73}\text{Ta}$	60.704	6.710×10^0	8.512×10^0	-0.93
$^{157}_{73}\text{Ta}$	60.893	1.516×10^{-1}	3.009×10^{-1}	-1.42
$^{159}_{75}\text{Re}$	60.408	7.792×10^{-6}	2.030×10^{-5}	-2.48
$^{160}_{75}\text{Re}$	60.712	1.633×10^{-4}	6.895×10^{-4}	-2.51
$^{161}_{75}\text{Re}$	60.864	1.269×10^{-4}	4.429×10^{-4}	-2.18
$^{161m}_{75}\text{Re}$	60.824	7.792×10^{-2}	2.238×10^{-1}	-2.50
$^{164}_{77}\text{Ir}$	60.598	4.171×10^{-5}	1.135×10^{-4}	-2.44
$^{165}_{77}\text{Ir}$	60.758	1.015×10^{-4}	3.395×10^{-4}	-2.71
$^{166m}_{77}\text{Ir}$	61.005	2.427×10^{-1}	8.465×10^{-1}	-2.70
$^{167}_{77}\text{Ir}$	61.207	2.117×10^{-2}	1.104×10^{-1}	-2.54
$^{167m}_{77}\text{Ir}$	61.154	2.132×10^0	7.507×10^0	-2.70
$^{171}_{79}\text{Au}$	61.140	4.105×10^{-6}	2.446×10^{-5}	-2.66
$^{176}_{81}\text{Tl}$	61.368	1.215×10^{-3}	5.196×10^{-3}	-2.33
$^{177}_{81}\text{Tl}$	61.514	2.242×10^{-2}	6.677×10^{-2}	-1.93

TABLE II. This table is similar to the previous one for the remaining seven emitters by presenting the used values of the nuclear radius parameter in the last column.

Nucleus	V_0^{Bech} (MeV)	$T_{\text{FM}}^{\text{calc}}$ (s)	$T_{\text{EM}}^{\text{calc}}$ (s)	ρ_s	r_0
$^{146m}_{69}\text{Tm}$	60.301	3.830×10^{-1}	2.029×10^{-1}	-2.58	1.291
$^{166}_{77}\text{Ir}$	61.062	6.310×10^{-2}	1.521×10^{-1}	-2.65	1.147
$^{170}_{79}\text{Au}$	61.017	1.530×10^{-6}	3.221×10^{-4}	-2.60	1.074
$^{170m}_{79}\text{Au}$	60.925	9.910×10^{-4}	1.052×10^{-3}	-1.77	1.070
$^{171m}_{79}\text{Au}$	61.060	2.180×10^{-3}	2.225×10^{-3}	-2.65	1.112
$^{177}_{81}\text{Tl}$	61.260	1.370×10^{-4}	3.988×10^{-4}	-2.60	1.010
$^{185}_{83}\text{Bi}$	61.861	3.310×10^{-5}	5.837×10^{-5}	-2.60	1.017

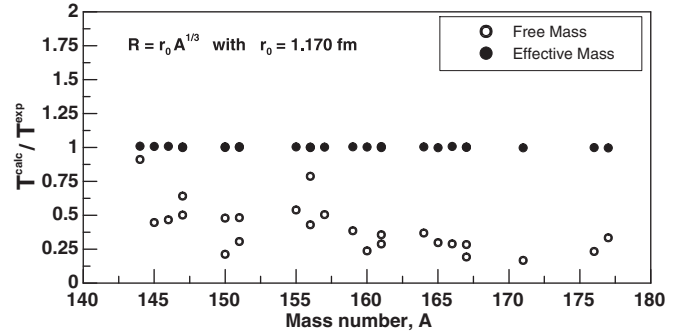


FIG. 2. This figure shows the ratio between calculated and experimental half-lives of proton emitters determined by using the free proton mass (small open circle) and including the effective mass correction (small full circle). Both calculations are carried out with no change in the parametrization of the shell potential [24]. These are results for the 25 emitters displayed in Table I.

Figs. 2 and 3 plots of the half-lives ratios values are shown. Here all values of $T_{\text{EM}}^{\text{calc}}$ are determined with no change in the potential parametrization [24]. All deviations of calculated results with respect to the experimental data are practically eliminated with the model improvement incorporating the effective mass correction, as shown in Figs. 2 and 3.

To reach the final half-lives values we have included in the calculation the effective mass correction for nuclei, the $T_{\text{EM}}^{\text{calc}}$ values in Tables I and II. In the first table (with 25 nuclei) are the emitters which permit half-life adjustments of $T_{\text{EM}}^{\text{calc}}$ values by changing only the effective mass parameter ρ_s without any change in the Becchetti parametrization of nuclear potential [24]. The ratio $T_{\text{EM}}^{\text{calc}}/T^{\text{exp}}$ obtained for these nuclei are plotted in Fig. 2, with a very strict adjustment. An error less than one percent of the mean experimental value of the half-lives was required, maintaining a variation in the ρ_s parameter (compatible with the one in Refs. [13,14]). We draw attention to the fact that even with this very rigorous criterion it is possible to adjust 25 emitters in a universe of 32 data, preserving the original potential parametrization.

The seven remaining emitters in Table II require additional small changes in the nuclear radius parameter r_0 in order

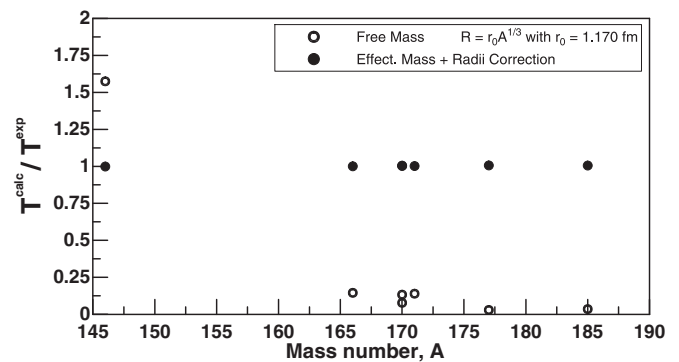


FIG. 3. These are results similar to the previous figure for the seven nuclei in Table II. The adjustments are done with the additional small change in nuclear radius parameter of the shell model potential, as it is shown in the last column of the table.

to maintain variations in the ρ_s compatible with those in Refs. [13,14]. In Fig. 3 the results of the ratio between calculated and experimental half-lives for these nuclei are shown. In the last column of Table II the values of the nuclear radius parameter used to achieve a better fit with the data are shown. Note that by considering the error bar of the half-life measurements, and also the error bar of the decay energy (Q values), the adjustment of the whole set with the change only in the ρ_s parameter is possible.

As it is shown in Table I, the calculation is able to adjust the half-lives for the majority of the studied nuclei with only one parameter, the ρ_s . A small number of almost spherical nuclei requires the change in nuclear radius systematic with a little variation of the nuclear radius parameter r_0 .

Here it is important to recognize that the introduction of a coordinate dependency in the proton effective-mass is a phenomenological manner to describe the proton-nucleus interaction inside the nucleus. The lack of an explicit treatment to the Pauli-exclusion principle in the proton evolution, as well as the absence of dynamical change of the mean field potential, generates the nonlocality feature of the potential. In general, to make the quantum many-body calculation viable,

the problem is reduced to an equivalent two-body problem using a time-independent effective mean field potential. The drastic reduction in the degree of freedom of the system with this mapping may introduce the necessity of a compensatory nonlocality feature in the interaction. In our case this characteristic of the nucleon-nucleus interaction is manifested with the velocity (or momentum) dependent term which is added to the coordinate dependent potential, when the form of the effective mass is incorporated into the Schrödinger equation, as demonstrated in Ref. [14].

Among many alternative approaches developed to determine half-lives of proton, α , and cluster emissions, some of them are based in the relativistic formulation of the nucleon-nucleus interaction. The main goal is to construct a mean field potential from a microscopic and more fundamental description of the nucleon interaction in the nuclear medium [25,26].

Finally we conclude that in spite of ρ_s being introduced in a phenomenological way, the nonlocality feature of the proton-nucleus interaction is able to correct discrepancies observed in the model calculation and half-life data of the proton emitters, with a desirable level of accuracy, by using an effective mass with a single parameter.

-
- [1] Chong Qi *et al.*, *Phys. Rev. C* **85**, 011303(R) (2012).
 [2] E. L. Medeiros *et al.*, *Eur. Phys. J. A* **34**, 417 (2007).
 [3] S. B. Duarte *et al.*, *At. Data Nucl. Data Table* **80**, 235 (2002).
 [4] P. J. Woods and C. N. Davids, *Annu. Rev. Nucl. Part. Sci.* **47**, 541 (1997).
 [5] O. A. P. Tavares and E. L. Medeiros, *Eur. Phys. J. A* **45**, 57 (2010).
 [6] E. Maglione, L. S. Ferreira, and R. J. Liotta, *Phys. Rev. Lett.* **81**, 538 (1998).
 [7] E. Maglione, L. S. Ferreira, and R. J. Liotta, *Phys. Rev. C* **59**, R589 (1999).
 [8] L. S. Ferreira and E. Maglione, *Phys. Rev. Lett.* **86**, 1721 (2001).
 [9] T. N. Leite, N. Teruya, and H. Dias, *Int. J. Mod. Phys. E* **11**, 469 (2002).
 [10] H. Feshbach, *Annu. Rev. Nucl. Sci.* **8**, 49 (1958).
 [11] W. E. Frahn and R. H. Lemmer, *Il Nuovo Cimento* **5**, 1564 (1957).
 [12] G. H. Rawitscher, *Phys. Rev. C* **31**, 1173 (1985).
 [13] M. I. Jaghoub, M. F. Hassan, and G. H. Rawitscher, *Phys. Rev. C* **84**, 034618 (2011).
 [14] R. A. Zureikat and M. I. Jaghoub, *Nucl. Phys. A* **916**, 183 (2013).
 [15] F. Perey and B. Buck, *Nucl. Phys.* **32**, 353 (1962).
 [16] O. von Roos, *Phys. Rev. B* **27**, 7547 (1983).
 [17] J. M. Lévy-Leblond, *Phys. Rev. A* **52**, 1845 (1995).
 [18] H. Feshbach, C. E. Porter, and V. E. Weisskopf, *Phys. Rev.* **96**, 448 (1954).
 [19] K. Kerman, H. McManus, and R. M. Thaler, *Ann. Phys. (NY)* **8**, 551 (1959).
 [20] R. Crespo, R. C. Johnson, J. A. Tostevin, R. S. Mackintosh, and S. G. Cooper, *Phys. Rev. C* **49**, 1091 (1994).
 [21] L. G. Arnold and B. C. Clarck, *Phys. Lett. B* **84**, 46 (1979).
 [22] L. S. Kisslinger, *Phys. Rev.* **98**, 761 (1955).
 [23] S. B. Duarte and N. Teruya, *Phys. Rev. C* **85**, 017601 (2012).
 [24] F. D. Becchetti and G. W. Greenlees, *Phys. Rev.* **182**, 1190 (1969).
 [25] M. Bhattacharya and G. Gangopadhyay, *Phys. Lett. B* **651**, 263 (2007).
 [26] Q. Zhao, J. M. Dong, J. L. Song, and W. H. Long, *Phys. Rev. C* **90**, 054326 (2014).